Proceedings of the 9ICEG
9th International Congress on Environmental Geotechnics
25-28 June, 2023 | Chania, Greece

https://doi.org/10.53243/ICEG2023-139

Effects of dry-wet cycles on the mechanical properties of sand treated with paper sludge ash-based stabilizer

Maliki Otieboame Djandjieme[1], Kimitoshi Hayano[2], Hiromoto Yamauchi [3]

[1]*PhD Candidate, Graduate School of Urban Innovation, Yokohama National University, 79-5 Tokiwadai, Hodogaya-ku, Yokohama 240-8501, Japan, maliki-djandjieme-mv@ynu.jp*

[2] *Professor, Faculty of Urban Innovation, Yokohama National University, 79-5 Tokiwadai, Hodogaya-ku, Yokohama 240-8501, Japan, hayano-kimitoshi-hg@ynu.ac.jp*

[3]*Coordinator, DOMI Environmental Solutions, 29 Minamisode, Sodegaura, Chiba 299-0268, Japan, yamauchi@domi-es.jp*

ABSTRACT

Backfill sand mixed with various additives changes the engineering properties during long-term variations in meteorological and hydrological conditions. Therefore, this paper aims to investigate the durability of Paper Sludge Ash-Based Stabilizer (PSAS)-treated sands subjected to dry-wet curing cycles. Two curing temperatures (40℃ and 71℃) were adopted for drying cylindrical specimens which were used for unconfined compression tests. In addition to the difference in the drying temperature, the effects of a number of dry-wet curing cycles on the unconfined compressive strength q_u were examined. The results showed an increase in the q_u of Paper sludge ash-treated sand at the early stage of the curing followed by a decrease in q_u with the curing process. However, the comparison of the unconfined compression test results with the cone index test results show that the confinement of the PSAS-treated sand can be an essential parameter for investigating the durability of PSAS-treated sands which were subjected to dry-wet curing cycles.

Keywords: paper sludge ash, backfill material, dry-wet curing cycles, strength development.

1 INTRODUCTION

The construction of public water supplies, waste acquisition systems, pipelines, and manholes generally require sand backfilling. However, backfilled sand typically exhibit weakness during significant natural events, such as earthquakes. In this context, weakness refers to the liquefaction phenomenon. When backfilled sand around underground pipes and manholes liquefy, it can cause a significant problem as their function is stopped, and they cannot be used during the period of recovery or damage restoration. This problem was observed during the Great East Japan earthquake in 2011 (Matsuhashi et al., 2014). According to Matsuhashi et al. (2014), immediately after the earthquake, 48 plants and 79 stations in sewage systems were shut down, and 63 plants and 32 stations were partially damaged. One year later, 2 plants and 12 stations remained shut down, while 12 plants and 25 stations remained partially damaged. Thus, the damage caused by liquefaction to underground pipes and manholes in sewage systems can significantly affect their function, and they cannot be used during the recovery or damage restoration period. To prevent such damage, backfilled sand is often enhanced with other materials to prevent liquefaction.

To date, various additives have been used to improve or stabilize backfilling sand, with conventional cement- and lime-based stabilizers being the most frequently used additives. Stabilizers can significantly increase the liquefaction strength of soils. Most soils treated with cement- or lime-based stabilizers demonstrate significant strength increase, even after 28 days of curing. However, excessive solidification over time may complicate re-excavation. Controlled Low-Strength Material (CLSM) can also be used as a substitute for compacted sand in backfill applications, but it has a limitation in installation, which requires achieving the required density homogeneously (Nataraja & Rao, 2016). In addition, the high alkalinity of cement or lime-soil mixtures is a concern (Imai et al., 2020; Inasaka et al., 2021). Furthermore, significant amounts of CO_2 emissions during the production of cement and lime are undesirable.

Soil stabilization using paper sludge ash-based stabilizer (PSAS) has been proposed recently (Kawai et al, 2018, Mochizuki, 2019, Phan et al., 2021, 2022). PSASs can be produced by insolubilizing heavy metals in original paper sludge (PS) ash particles, which is waste generated by the incineration of PS discharged from paper mills (Watanabe et al., 2021, Phan et al., 2021, 2022, Tabassum et al., 2022). The manufacture of PSASs from PS ash emits less CO_2 than that of cement- or lime-based stabilizers because PS ash is not generated as an end product but as an industrial waste (Trung et al., 2021, 2022).

Recently, authors have reported that unconfined compressive strength - q_u of PSAS-treated sands was lower than that of Ordinary Portland Cement (OPC)-treated sands under the same mixing conditions, even though the oxide components of the PSAS was similar to that of OPC. The increase in q_u with curing time was more gradual in the PSAS-treated sands than in the OPC-treated sands, suggesting that the former is easier to be re-excavated. In addition, authors have also demonstrated that the pH of PSAS-treated sands could be lower than that of OPC-treated sands (Djandjieme et al., 2022).

However, durability of PSAS-treated sands has not been investigated in detail so far. Therefore, this paper aims to investigate the durability of PSAS-treated sands which were subjected to dry-wet curing cycles. Two curing temperature (40℃ and 71℃) were adopted for drying cylindrical specimens which were used for unconfined compression tests. In addition to the difference in the drying temperature, the effects of numbers of dry-wet curing cycles on the q_u were examined. Moreover, dry-wet curing cycles were given to cone index specimens to compare the test results with the unconfined compression test results. The effect of the confinement of the PSAS-treated sands on the durability for dry-wet curing cycles will be discussed.

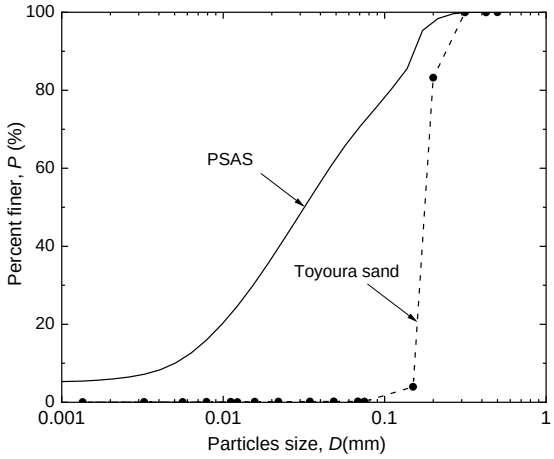

Figure 1. *Particle size distributions of Toyoura sand and PSAS*

Table 1. *Oxide components of PSAS and OPC (%: mass ratio)*

(a) PSAS

CaO	SiO_2	Al_2O_3	SO_3	FeO	MgO	P_2O_5	Others
63.89	13.55	6.89	6.06	3.27	1.31	0.95	4.08

(b) OPC

CaO	SiO_2	Al_2O_3	SO_3	FeO	MgO	P_2O_5	Others
65.57	19.07	5.26	3.98	2.91	1.98	0.25	0.92

2 MATERIALS AND EXPERIMENT DESIGN

2.1 Materials

The materials used in this study are Toyoura sand, PSAS, OPC. The unified soil classification system (USCS) classifies Toyoura sand as a poorly graded sand, with a particle density, ρ_s = 2.641 g/cm^3. The particle size distribution (PSD) of Toyoura sand is shown in Figure 1 The PSAS is a commercial product available in Japan, whose particle density ρ_s is 2.603 g/cm^3. The PSD of the PSAS could not be evaluated based on the Japanese Geotechnical Society standard JGS 0131 due to its hydration reaction, therefore, the PSD shown in fig.1 was obtained using laser diffraction analyses with anhydrous

ethanol instead of water as a medium in the analyses. Furthermore, OPC with a particle density ρ_s of 3.15 g/cm^3 was used as a stabilizer for treating the sand and then compared with PSAS-treated sand. The oxide components of the PSAS and OPC (%: mass ratio) obtained via X-ray fluorescence analysis are listed in Table 1.

The oxide components of the PSAS were found to be similar to that of OPC, specifically in terms of the amount of calcium oxide (CaO) present, as shown in table 1. PSAS contained approximately 63.9%CaOby mass, which allowed it to undergo a hydration reaction when mixed with water. However, the strength of this reaction was found to be inferior to that of cement, as OPC is mainly composed of calcium silicates while PSAS is composed of a mixture of oxides and minerals including silica (Phan et al., 2021).

The pH value of PSAS was determined to be 11.7, which was lower than the pH of OPC (12.7). this difference in pH value could have an impact on the behaviour and performance of the materials in various applications.

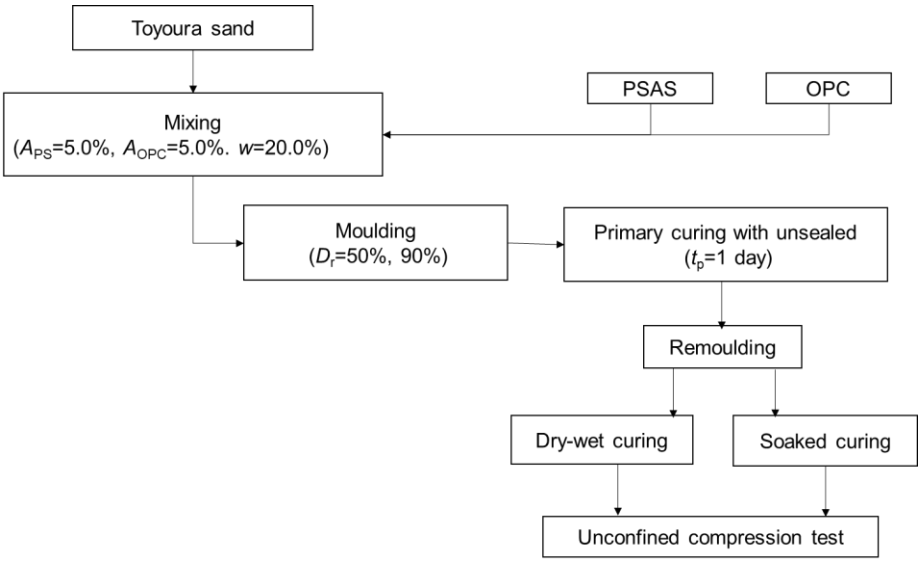

Figure 2. *Specimen preparation flow for unconfined compression test of treated specimens*

2.2 Specimen preparation

For unconfined compression test specimen preparation, dry Toyoura sand was first mixed with the PSAS with A_{PS} = 5.0% The A_{PS} was the dry mass ratio of PSAS to Toyoura sand. Immediately after mixing, the water content w of the treated sand was adjusted to 20% as appropriate mixture conditions to prevent the excessive expansion of treated sand and an overly high water content (Djandjieme et al., 2022).Thus, the mixtures were placed into cylindrical plastic molds (50 mm in diameter and 100 mm in height) and compacted to achieve D_r = 50% and 90%; the molds were exposed to air-precuring for t_p=1 days before it is remolded for dry-wet cycle process shown in Figure 2. For comparison, OPC-treated sand specimens with A_{OPC} = 5.0% were prepared under the same condition. The A_{OPC} was the dry mass ratio of OPC to Toyoura sand.

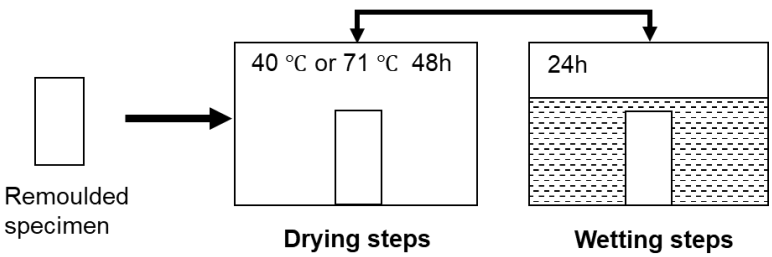

Figure 3. *Schematic experimental process of the cycling drying-wetting treated specimens.*

2.3 Experimental design of dry and wet curing cycle

The presence of dry-wet curing cycles is considered as one of the aggressive environmental conditions experienced by soils. In this study, the indoor dry and wet cycle environment was simulated as shown in Figure 3. The PSAS- and OPC-treated sand specimens were dried for 48h in an oven at temperature of 40℃ or 71℃. Subsequently, they were immersed in the water and left for 24h in the room temperature. The drying and wetting process was repeated. The mass of each specimen was measured associated with the drying and wetting curing cycles, and the change in the saturation degree was calculated. Figure 4 shows the examples of the change in the saturation degree with cycles. Finally, unconfined compression tests were carried out on the treated sand specimens with 1,2,3,4,5,6 and 7 cycles.

3 UNCONFINED COMPRESSIVE STRENGTH OF TREATED SPECIMENS CURED UNDER DRY-WET CYCLE AND SOAKED CONDITIONS

Unconfined compressive strength q_u of PSAS-treated specimens is shown in Figure. 5. The q_u of PSAS-treated specimens subjected to continuous soaked curing increased with the curing period. However, the q_u of PSAS-treated specimens subjected to dry-wet curing cycles increased at the initial stage of the curing, and then, the q_u decreased towards zero after several cycles of dry-wet curing. In Figure 6 where q_u of OPC-treated sand at 5% mixture ratio is plotted against the curing period, the q_u of treated specimen increased from the 1st to 7th cycle for each curing condition. The q_u of OPC-treated sand specimens demonstrates the importance of considering higher temperature during the curing process under dry-wet cycles. When specimens were cured at T=40℃, Figure 6 clearly shows that the q_u of OPC-treated sand under soaked conditions was lower than the q_u obtained under dry-wet cycles. At T=71℃, there was a disruption in the q_u value obtained when number of the dry-wet curing cycles increased. This might be because moderately high temperatures accelerated the hydration reaction, whereas excessively high temperatures might also cause loss of hydrates.

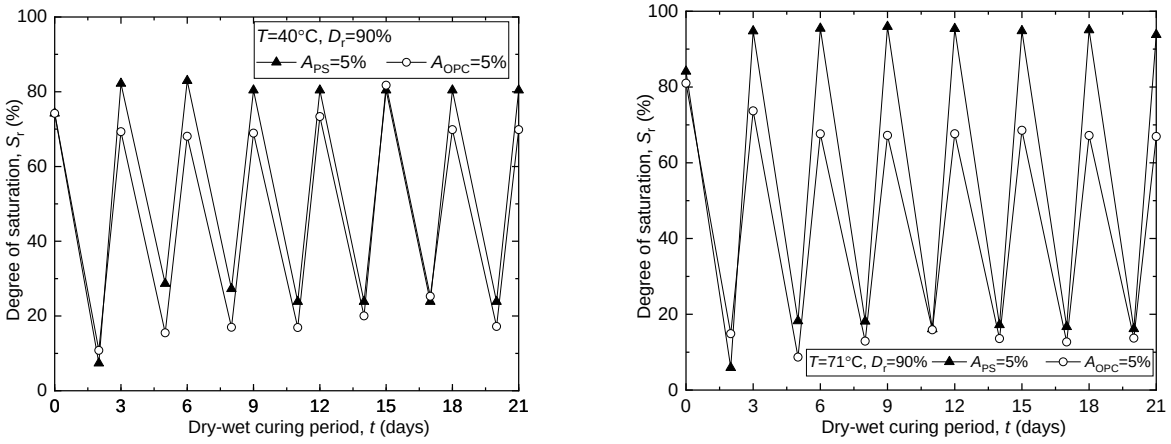

(a) T=40℃ (b) T=71℃

Figure 4. *Change in saturation degree of PSAS and OPC treated sand during dry-wet curing.*

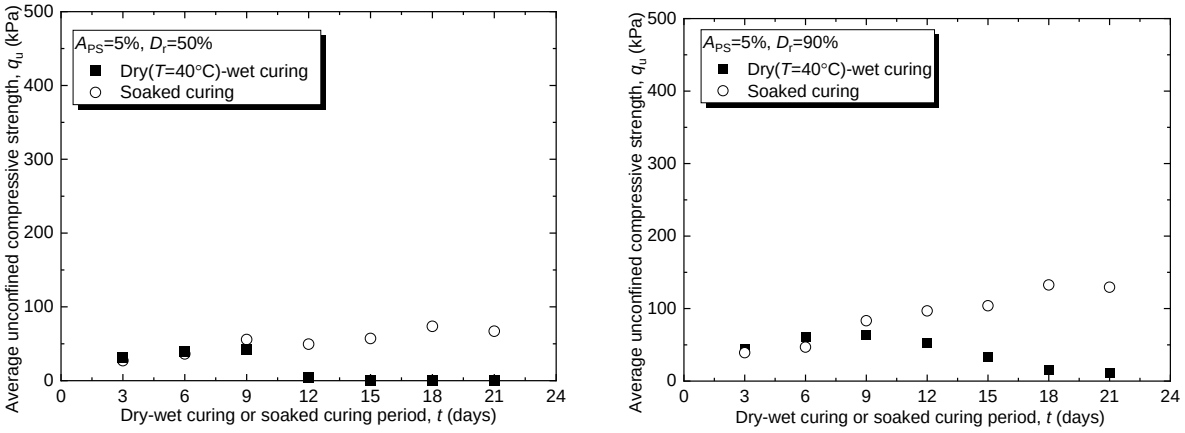

(a) PSAS-treated sand at Dr=50%, T=40℃ *(b) PSAS-treated sand at Dr=90%, T=40℃*

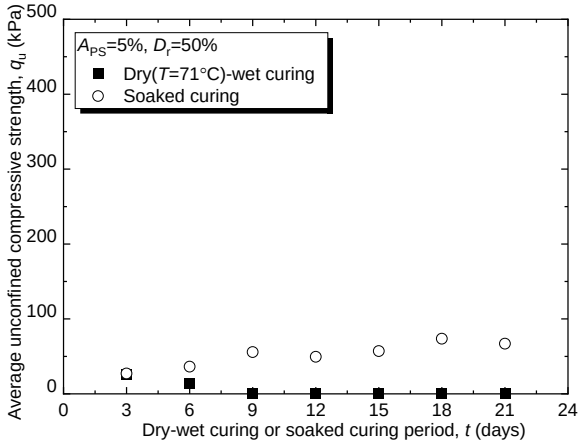

(c) PSAS-treated sand at Dr=50%, T=71℃

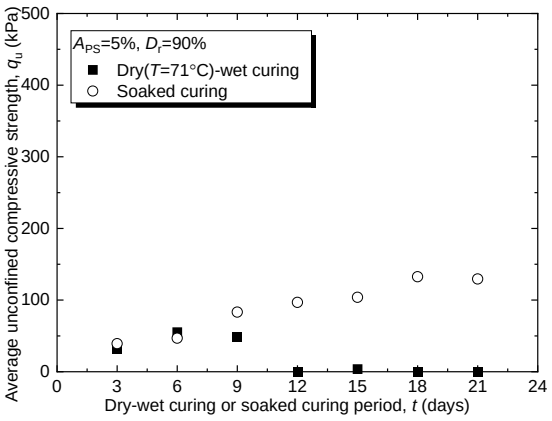

(d) PSAS-treated sand at Dr=90%, T=71℃

Figure 5. *Relationships between unconfined compressive strength q_u and curing period under dry-wet cycle and soaked conditions for PSAS-treated sand.*

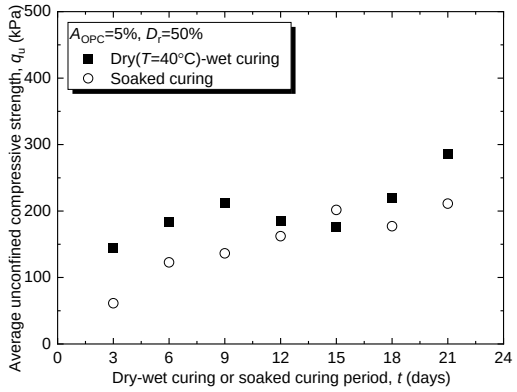

(a) OPC-treated sand at Dr=50%, T=40℃

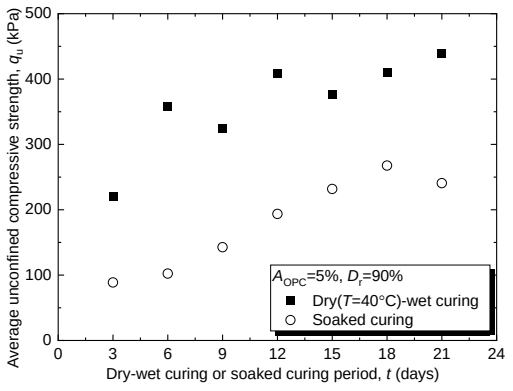

(b) OPC-treated sand at Dr=90%, T=40℃

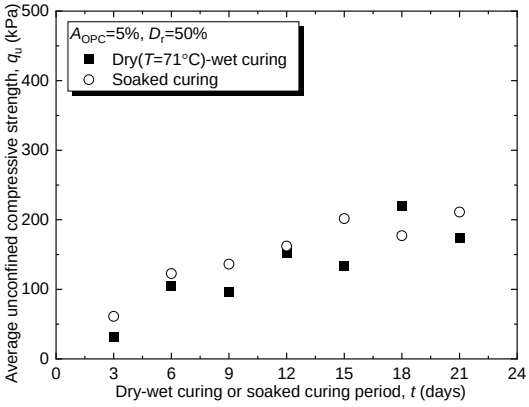

(c) OPC-treated sand at Dr=50%, T=71℃

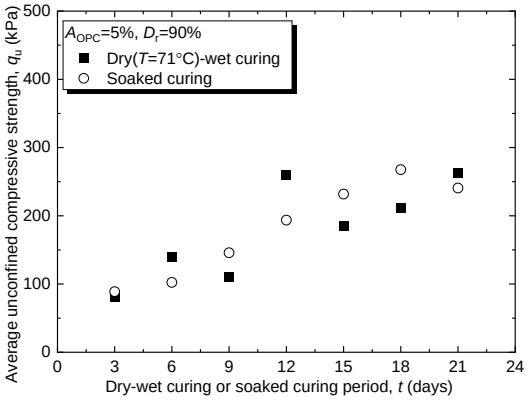

(d) OPC-treated sand at Dr=90%, T=71℃

Figure 6. *Relationships between unconfined compressive strength q_u and curing period under dry-wet cycle and soaked conditions.*

4 COMPARISON OF STRENGTH DEVELOPMENT OBTAINED FROM CONE INDEX TEST AND UNCONFINED COMPRESSION TEST

The Cone index test is a widely used method in Japan for determining the cone index of compacted treated soils. This test involves the use of a cone penetrometer equipped with a a tip cone, a rod, a jack for penetrating, and a load cell. To obtain the cone index value, the average force acting on the cone is divided by the bottom area of the tip cone when it has penetrated 5 cm, 7.5 cm, and 10 cm from the top surface of the specimen. In this study, cone index tests were performed on PSAS-treated samples cured

under dry-wet cycles, and the results were compared with those of unconfined compression tests to investigate the effect of confinement on the strength development. The specimen for the cone index test was prepared following the Japanese geotechnical society standard for cone index test on compacted soil (JGS 0716 & 0711). The dry and wet cycle environment were simulated such that the specimen was dried for 48h in an oven at temperature of 71℃ and soaked in water for one day.

Figure 7(a) shows the change in the saturation degree with the dry-wet curing cycle. Figure 7(b) shows the relationship between the cone penetration resistance and the cone penetration of each specimen. The cone penetration resistance increased from the 1st to the 3rd cycle. Followingly, the cone penetration resistance decreased with the increase in the number of dry-wet curing cycle. However, the cone penetration resistance obtained at the 7th cycle was significantly higher than that of untreated specimen. The test results suggested that the confinement was essential to precisely assess the durability of the PSAS-treated sands subjected to dry-wet curing.

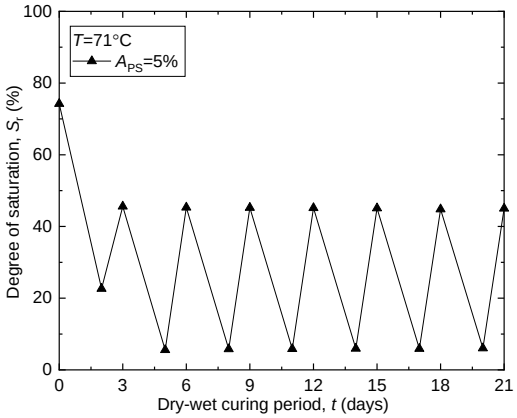

***(a)** Saturation table of PSAS treated sand under dry-wet cycle*

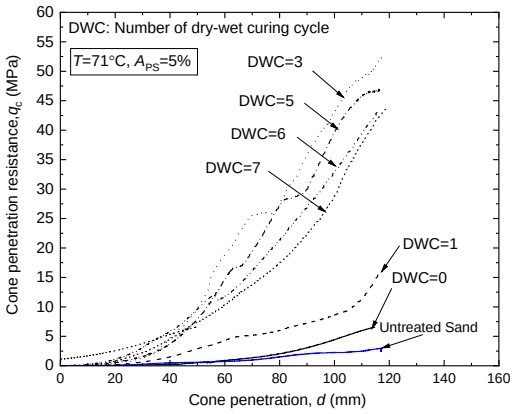

***(b)** Cone index test of PSAS treated sand under dry-wet cycle*

***Figure 7.** q_c of PSAS treated sand under dry-wet cycle*

.

5 XRD PROFILE OF PSAS-TREATED SAND SUBJECTED TO DRY-WET CURING

The q_u of the PSAS-treated sand increased gradually at the initial stage of the curing and then decreased as number of the dry-wet curing cycles increased, as described in the previous section. Then, the investigation of the crystalline substance was conducted to understand the hydration process during the dry-wet cycle by conducting XRD diffraction tests. XRD analyses were conducted on PSAS-treated sands after the 1st, 4th and 5th cycle (C1, C4 and C5) of dry-wet curing. The PSAS-treated sands were dried for 48h in an oven-dry at temperature of 71℃. Subsequently, they were immersed below the water surface and left for 24h in the room temperature. After the prescribed dry-wet cycle curing at C1, C4, and C5, PSAS-treated sand was crushed in a ceramic mortar using a pestle and soaked in iso-propanol for 2h. Next, vacuum filtration was performed to remove the alcohol, and the sample was placed in a vacuum oven set to 40°C for 1 day. Immersing treated sand in alcohol halted the hydration reaction. The treated sand was passed through a 0.075 mm sieve and was used for X-ray powder diffraction in a Rigaku Ultima IV D-5000 Diffractometer using Cu K-alpha radiation. The diffractometer was collected in the range of 20-60° 2θ Scale, with a step size of 0.005°/sec.

The XRD profiles of the treated sand under dry-wet cycles are presented in Figure 8. The XRD profiles of the PSAS before the hydration are also presented in the figure. The Ettringite was present at C1, and the counts were decreased as the dry-wet cycles increased (at C4 and C5). This ettringite counts change might have contributed to the observed change in q_u of the PSAS-treated sands. At a high temperature one component of Ettringite transforms to monosulphate just like concrete at a very early stage of hydration (Nanayakkara, 2011). Therefore, in Figure 8 we can easily see the decrease of the Ettringite peak after fourth cycle, which can be justified by the instability of Ettringite at high temperature(>70°C). In detail, one observes that samples exhibited the presence of Calcium oxide and Calcium sulfate components after fourth cycles. So, the presence of Calcium sulfate can be expressed by the reaction of the calcite $CaCO_3$ with Sodium sulfate Na_2SO_4.

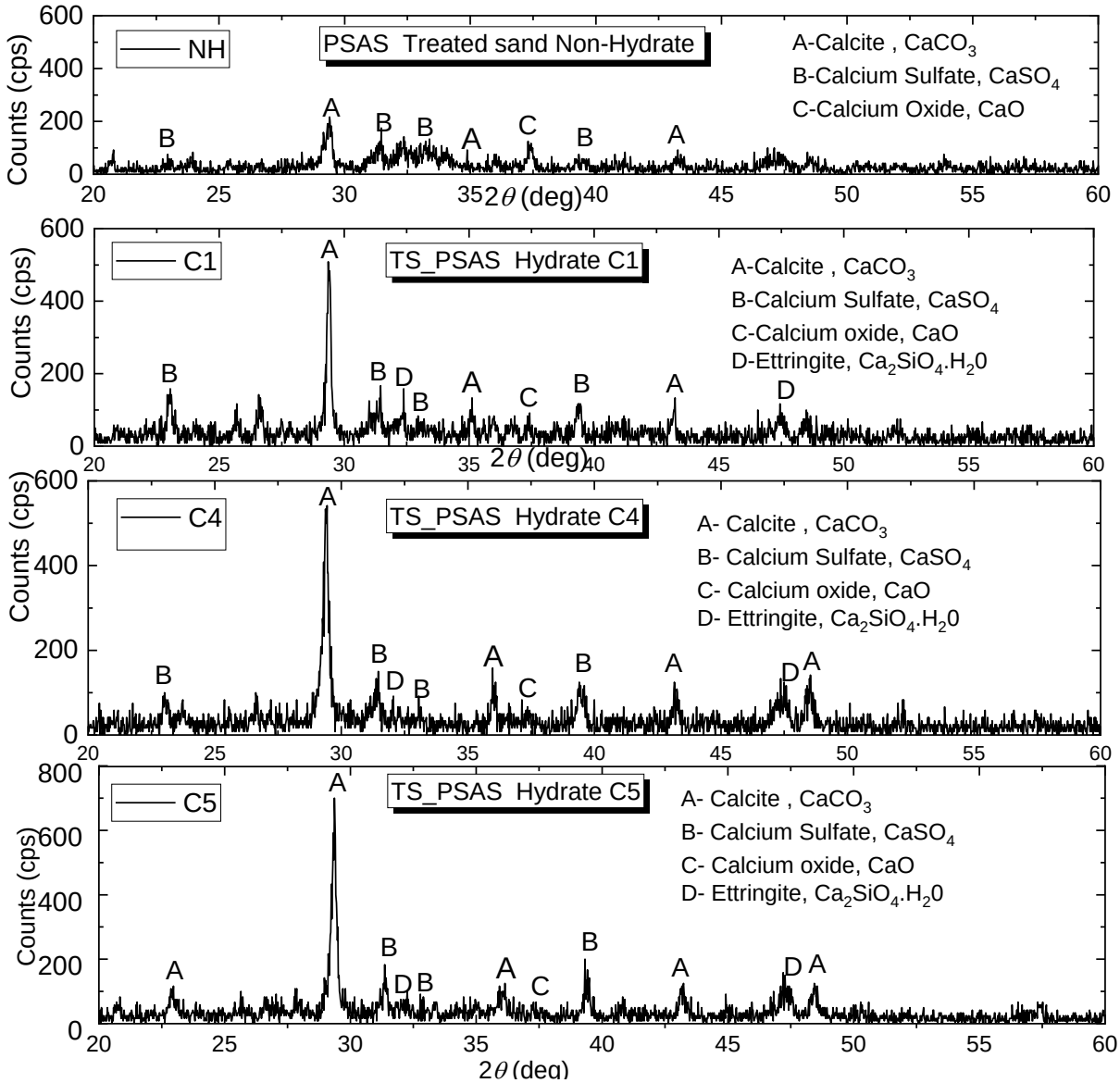

Figure 8. *XRD Profiles of PSAS treated sand at each dry-wet cycle conditions.*

6 CONCLUSIONS

In this study, the durability of PSAS-treated sands subjected to dry-wet cycles as a backfill material around underground pipes was investigated.

The following conclusions were obtained:

1. The q_u of PSAS-treated specimens subjected to dry-wet cuing cycles increased at the initial stage of the curing, and then, the q_u decreased towards zero after several cycles of dry-wet curing. Meanwhile, the q_u of OPC-treated sand increased with the increase in the number of dry-wet curing cycle.
2. However, the cone penetration resistance of the PSAS-treated specimens subjected to dry-wet cuing cycles was significantly higher than that of untreated specimen. The test results suggested that the confinement was essential to precisely assess the durability of the PSAS-treated sands subjected to dry-wet curing.
3. The XRD profiles of the PSAS- treated sand under dry-wet cycles demonstrated that ettringite content present during the first cycle decreased as the dry-wet cycles increased, owing to the instability of Ettringite at high temperature (>70°C).

7 ACKNOWLEDGEMENTS

This work is supported by Japanese Government (MEXT) scholarship.

REFERENCES

Matsuhashi, M., Tsushima, I., Fukatani, W., & Yokota, T. (2014). Damage to sewage systems caused by the Great East Japan Earthquake, and governmental policy. Soils and Foundations, 54(4), 902-909.

Nataraja, M. C., & Rao, N. V. (2016). Controlled low strength material with fly ash and cinder aggregates: an effective replacement for the compacted backfill. Indian Journal of Advances in Chemical Science S1, 289, 293.

Imai, K., Hayano, K., & Yamauchi, H. (2020). Fundamental study on the acceleration of the neutralization of alkaline construction sludge using a CO2 incubator. Soils and Foundations, 60(4), 800-810.

Inasaka, K., Trung, N. D., Hayano, K., & Yamauchi, H. (2021). Evaluation of CO2 captured in alkaline construction sludge associated with pH neutralization. Soils and Foundations, 61(6), 1699-1707.

Kawai, S., Hayano, K., & Yamauchi, H. (2018). Fundamental study on curing effect and its mechanism on the strength characteristics of PS ash-based improved soil. Journal of Japan Society of Civil Engineers, Ser. C (Geosphere Engineering), 74(3), 306-317.

Jayawardane, V. S., Anggraini, V., Li-Shen, A. T., Paul, S. C., & Nimbalkar, S. (2020). Strength Enhancement of Geotextile-Reinforced Fly-Ash-Based Geopolymer Stabilized Residual Soil. International Journal of Geosynthetics and Ground Engineering, 6(4), 50. https://doi.org/10.1007/s40891-020-00233-y

Mochizuki, Y. (2019). Evaluation of water absorption performance of various PS ashes produced with different incineration methods and its applicability for mud improvement. Japanese Geotechnical Society Special Publication, 155–166.

Nanayakkara, S. M. A. (2011). Importance of controlling temperature rise due to heat of hydration in massive concrete elements. http://dl.lib.uom.lk/handle/123/12394

Djandjieme, M., Hayano, K., Yamauchi, H., & Maqsood, Z. (2022). Swelling and strength characteristics of sand treated with paper sludge ash-based stabilizer. Construction and Building Materials, 341, 127849. https://doi.org/10.1016/j.conbuildmat.2022.127849

Phan, N.B., Hayano, K., Mochizuki, Y., Yamauchi, H. (2021). Mixture design concept and mechanical characteristics of PS ash–cement-treated clay based on the water absorption and retention performance of PS ash. Soils and Foundations, 61(3), 692–707.

Phan, B. N., Sekine, R., Hayano, K., & Yamauchi, H. (2022). Assessment of consistency and strength properties of clays treated with paper sludge ash-based stabilizers using the water absorption and retention rate. Construction and Building Materials, 351, 128936.

Pinkert, S., & Hayley, J. (2016). Experimental verification of a prediction model for hydrate bearing sand: Verification of hydrate prediction model. Journal of Geophysical Research: Solid Earth, 121. https://doi.org/10.1002/2015JB012320

Tabassum, N., Hashino, T., Phan, B.N., Hayano, K. and Yamauchi, H. (2022). Effects of primary curing conditions and subsequent crumbling on properties of compacted soils treated with paper sludge ash-based stabilizers. Soils and Foundations, 62(5):101183.

Trung, N. D., Ogasawara, T., Hayano, K., & Yamauchi, H. (2021). Accelerated carbonation of alkaline construction sludge by paper sludge ash-based stabilizer and carbon dioxide. Soils and Foundations, 61(5), 1273-1286.

Trung, N. D., Hayano, K., & Yamauchi, H. (2022). Effects of sample crumbling and particle size on accelerated carbonation of alkaline construction sludge treated with paper-sludge ash-based stabilizers. Soils and Foundations, 62(6), 101239. 6.

Watanabe, Y., Binh, P. N., Hayano, K., & Yamauchi, H. (2021). New mixture design approach to paper sludge ash-based stabilizers for treatment of potential irrigation earth dam materials with high water contents. Soils and Foundations, 61(5), 1370-1385.